Free Radical Research, June 2007; 41(6): 615–626

informa
healthcare

Platinum nanoparticle is a useful scavenger of superoxide anion and hydrogen peroxide

MASASHI KAJITA[1,2], KEISUKE HIKOSAKA[1], MAYUMI IITSUKA[2], ATSUHIRO KANAYAMA[1], NAOKI TOSHIMA[3], & YUSEI MIYAMOTO[1]

[1]*Department of Integrated Biosciences, Graduate School of Frontier Sciences, University of Tokyo, Chiba, Japan,* [2]*APt Co., Ltd., Tokyo, Japan, and* [3]*Department of Materials Sciences and Environmental Engineering, Tokyo University of Science in Yamaguchi, Yamaguchi, Japan*

Accepted by Dr E Niki

(Received 10 July 2006; in revised form 13 December 2006)

Abstract
Bimetallic nanoparticles consisting of gold and platinum were prepared by a citrate reduction method and complementarily stabilized with pectin (CP-Au/Pt). The percent mole ratio of platinum was varied from 0 to 100%. The CP-Au/Pt were alloy-structured. They were well dispersed in water. The average diameter of platinum nanoparticles (CP-Pt) was 4.7 ± 1.5 nm. Hydrogen peroxide (H_2O_2) was quenched by CP-Au/Pt consisting of more than 50% platinum whereas superoxide anion radical (O_2^-) was quenched by any CP-Au/Pt. The CP-Au/Pt quenched these two reactive oxygen species in dose-dependent manners. The CP-Pt is the strongest quencher. The CP-Pt decomposed H_2O_2 and consequently generated O_2 like catalase. The CP-Pt actually quenched O_2^-, which was verified by a superoxide dismutase (SOD) assay kit. This quenching activity against O_2^- persisted like SOD. Taken together, CP-Pt may be a SOD/catalase mimetic which is useful for medical treatment of oxidative stress diseases.

Keywords: *Bimetallic nanoparticles, platinum, gold, reactive oxygen species, catalytic quencher, superoxide dismutase/catalase mimetic*

Introduction

Metal nanoparticles have been developed to increase the catalytic activity of metals due to the larger surface area of smaller particles. To achieve their reliable high catalytic activity, synthetic chemists have made great efforts towards establishing new preparation methods to control their size, structure, composition and dispersibility [1–4]. Many preparation techniques using diverse metal sources have been developed. The developed techniques are broadly classified into two types, chemical and physical methods. Chemical methods are more popular than physical ones because the former methods are easy to control the size and also suitable for mass production. Chemical methods consist of two concurrent reaction steps, reduction of metal salts or precursors to metal atoms and control of aggregation of metal atoms with stabilizers. Typical reactions catalyzed by metal nanoparticles so far reported are hydrogenation, hydration, oxidation and so on [1,5–9]. Furthermore, metal nanoparticles exhibit such as electric, magnetic and thermodynamic properties because of a high ratio of metal atoms lying on the surface, which enables us to develop their new application other than use as catalysts [10–14]. In the biological application of metal nanoparticles, gold nanoparticles have been mainly used as nanoprobes for transmission electron microscope (TEM) [15]. Since some noble metal nanoparticles are reducing catalysts, they may be usable as antioxidants which

Correspondence: Y. Miyamoto, Department of Integrated Biosciences, Graduate School of Frontier Sciences, University of Tokyo, Bioscience Building 402, 5-1-5 Kashiwanoha, Kashiwa, Chiba 277-8562, Japan. Tel: 81 4 7136 3628. Fax: 81 4 7136 3630. E-mail: yusei74@k.u-tokyo.ac.jp

ISSN 1071-5762 print/ISSN 1029-2470 online © 2007 Informa UK Ltd.
DOI: 10.1080/10715760601169679

reduce reactive oxygen species (ROS) in a living body. However, there are only a few studies reporting antioxidant effects of gold nanoparticles [16–18].

Typical ROS in animals including human being are superoxide anion radical (O_2^-), hydrogen peroxide (H_2O_2) and hydroxyl radical ($^{\cdot}OH$) produced in normal metabolic pathways [19]. The dominant pathway to generate ROS is the mitochondrial electron transport chain, by which approximately 98% of oxygen inhaled by animals is stepwise reduced to water for energy production. In this electron transport process, a small number of electrons leak out and directly react with oxygen to generate O_2^- as a byproduct [20]. The O_2^- is reduced to H_2O_2 by superoxide dismutase (SOD), and subsequently H_2O_2 goes across the mitochondrial membranes and diffuse inside and even outside of cells. The $^{\cdot}OH$ is generated from O_2^- and H_2O_2 by Haber-Weiss and Fenton reactions, respectively. These ROS oxidize biomolecules composing the body such as lipids, proteins and nucleic acids. There are many defensive systems against oxidative stress in the body [21]. As the first defence, ROS are reduced by antioxidant enzymes such as SOD, catalase and glutathione peroxidase as well as endogenous and exogenous small molecules including glutathione, vitamin C and E. When biomolecules are oxidized, they are repaired or replaced by biological protective systems. Nevertheless, biomolecules are irreversibly oxidized little by little and oxidized biomolecules accumulate as time goes by and impair biological functions, eventually leading to aging and age-related diseases [22,23].

On the other hand, ROS are also useful biological substances in the body. They function as cellular signaling molecules [24–26] and also take part in the host defence to kill invaded bacteria, viruses and funguses [27]. To accomplish these functions, the appropriate regulation of ROS concentrations is required. When ROS are excessively generated or biological antioxidant defense systems are suppressed in the body, increase of ROS causes oxidative tissue injury and is implied in the pathogenesis of different types of diseases including inflammation and neurodegeneration [23].

Previous reports had shown that platinum nanoparticles containing a certain amount of additional other metals such as palladium and gold exhibit higher catalytic activity in hydrogenation and hydrogen evolution than platinum monometallic nanoparticles [28,29]. Thus, we tried to manufacture platinum bimetallic nanoparticles to examine the quenching activity against ROS. Gold was chosen as a partner metal, because it was well known that cysteine residues in peptides stably bind to the surface of gold through thiol groups by means of coordination and hence gold in metal nanoparticles seemed to be useful to bind some functional peptides to their surface in future biological experiments. Therefore, in the present study, we made an investigation on antioxidant properties of bimetallic nanoparticles consisting of gold and platinum which were prepared by a citrate reduction method. Their quenching activity and properties against H_2O_2 and O_2^- will be described.

Materials and methods

Materials

Hydrogen hexachloroplatinate hexahydrate ($H_2PtCl_6{\cdot}6H_2O$), hydrogen tetrachloroaurate tetrahydrate ($HAuCl_4{\cdot}4H_2O$), trisodium citrate dihydrate, H_2O_2, hypoxanthine (HPX), L-ascorbic acid, tannic acid, uric acid, platinum black (Pt-black) and catalase were purchased from Wako Pure Chemical Industries, Ltd. (Osaka, Japan). Catechin hydrate was purchased from Sigma-Aldrich Co. (St Louis, MO, USA). Pectin was generously provided by Unitec Foods Co., Ltd. (Tokyo, Japan). Xanthine oxidase (XOD) was obtained from Roche Diagnostics Corporation (Indianapolis, IN, USA). 5,5-Dimethyl-1-pyrroline-*N*-oxide (DMPO) was from Labotec Ltd. (Tokyo, Japan). A SOD assay kit-WST was from Dojindo Laboratories (Kumamoto, Japan). All other reagents were of the highest grade commercially available. Water was freshly prepared with a Millipore Milli-Q academic (Millipore, Billerica, MA, USA).

Preparation of noble metal nanoparticles

Bimetallic nanoparticles consisting of gold and platinum were prepared by a citrate reduction method according to a previous report with miner modification [30]. Citrate works not only as a reducing but also protecting reagent. To improve the stability of noble metal nanoparticles, pectin was used as an additional protecting reagent. Consequently, bimetallic nanoparticles consisting of gold and platinum protected with citrate and pectin (CP-Au/Pt) were manufactured. In brief, 43.8 ml of water was placed in a 100 ml eggplant type flask and 4 ml of the mixture of two aqueous solutions containing noble metal ions, 16.6 mM $H_2PtCl_6{\cdot}6H_2O$ and 16.6 mM $HAuCl_4{\cdot}4H_2O$, was added. By changing the volume rates of these two noble metal ion solutions, the percent mole ratio of gold to platinum (Au:Pt) was varied as follows: 0:100, 25:75, 50:50, 75:25 and 100:0. The reaction mixture in the flask was stirred at 100°C till reflux started. Then, 8.6 ml of 77.2 mM trisodium citrate dihydrate was injected to the reaction mixture and the reflux was continued for additional 30 min. The color change of the reaction mixture from light yellow to dark brown or dark red was watched to know the start of noble metal ion reduction and the progression of their nanoparticle formation. After the reaction mixture was cooled down to the room temperature, 10 ml of 3.96 mg/ml pectin was added and stirring was continued for another hour. In any CP-Au/Pt with

varied gold and platinum mole ratios, the concentrations of total noble metals, citrate and pectin were 1 mM, 10 mM and 0.6 mg/ml in the resultant mixture, respectively. This concentration ratio was determined to obtain the best stability of CP-Au/Pt in 0.9% NaCl solution in water. In this paper, the values of Au:Pt of CP-Au/Pt represent those calculated from $HAuCl_4 \cdot 4H_2O$ and $H_2PtCl_6 \cdot 6H_2O$ used in preparation.

Characterization of CP-Au/Pt

Ultraviolet and visible (UV–Vis) spectra of CP-Au/Pt were measured by Ultrospec 6300 pro spectrophotometer (GE Healthcare Bio-Science Corp., Uppsala, Sweden) to monitor fading of the absorption specific to noble metal precursor ions and appearance of the surface plasmon absorption specific to noble metal nanoparticles [29]. The concentration of total noble metals in CP-Au/Pt was diluted to 200 μM.

The contents of gold and platinum composing CP-Au/Pt manufactured were analyzed by inductively coupled plasma atomic emission spectrometry (ICP-AES) using SPS4000 (SII NanoTechnology Inc., Tokyo, Japan). To estimate the constituent mole ratio of gold and platinum on the surface of CP-Au/Pt and also to examine platinum state, atomic, ionized or oxygenated, on the surface of CP-Au/Pt and Pt-black, X-ray photoelectron spectroscopy (XPS) was performed using dried CP-Au/Pt on the filter and Pt-black powder. The instrument for XPS employed was ESCALAB220iXL (Thermo Electron Co., Waltham, MA, USA). A monochromatic Al $K_{\alpha 1,2}$ line ($h\nu = 1486.6$ eV) was used. A take-off angle was 90°.

Electron micrographs were taken by H-7600 TEM manufactured by Hitachi Science Systems Ltd. (Tokyo, Japan). Its operating conditions were 100 kV of the acceleration voltage and 120,000 of the magnification. The copper mesh was used as a support grid for CP-Au/Pt. The concentration of total noble metals in CP-Au/Pt was 1 mM. The diameter of each particle of CP-Au/Pt in enlarged photographs was measured using a magnifying loupe (Tohkai Sangyo Co., Ltd., Tokyo, Japan) [7]. The histogram of the particle size distribution and the average diameter were obtained from the measurements of 200 particles.

Quenching of H_2O_2

The concentration of H_2O_2 was determined by a spectrophotometrical method [31]. In brief, 2880 μl of 20 mM H_2O_2 was placed in a quartz cuvette and 120 μl of a sample solution in water containing one of CP-Au/Pt, citrate, pectin, L-ascorbic acid, catechin and Pt-black was added to initiate quenching of H_2O_2. After 5 min incubation, the concentration of residual H_2O_2 was calculated from absorbance measured at 240 nm by the spectrophotometer. The absorbance of 120 μl of each corresponding sample solution diluted with 2880 μl of water was subtracted as a blank because the absorption change in this assay is specific for hydrogen peroxide under the condition. Water was used as a vehicle control and residual H_2O_2 was expressed as percentage of the control.

Quenching of O_2^-

Quenching of O_2^- by CP-Au/Pt was measured using a spin-trapping technique with an electron spin resonance (ESR) system, JES-FA 100 (JEOL, Tokyo, Japan) [32]. As a spin-trapping reagent DMPO was used and consequently the O_2^- adduct (DMPO-OOH) was monitored by ESR. The O_2^- was generated by an enzymatic reaction with HPX and XOD. The reaction was initiated with adding 50 μl of 0.2 U/ml XOD in 200 mM phosphate buffer (pH 7.5) to a mixture of 15 μl of 8.8 M DMPO, 50 μl of 5.5 mM HPX in 200 mM phosphate buffer (pH7.5) and 100 μl of one of the sample solution in water. The DMPO—OOH signal was measured at 45 s after the addition of XOD. The conditions for ESR measurement were as follows: field, 335.6 ± 5 mT width; power, 4 mW; field modulation, 100 kHz and 0.08 mT; time constant, 0.03. The manganese signal was used as an external standard of ESR signal and the intensity of DMPO—OOH signal was normalized by that of the manganese signal to convert to the numeric value. Water was used as a vehicle control and the converted numeric values of DMPO—OOH signal representing residual O_2^- were expressed as percentage of the control.

Quenching of O_2^- by CP-Pt was also estimated by a different method, formazan formation using a SOD assay kit-WST. The O_2^- was generated by the enzymatic reaction with xanthine and XOD. The assay was performed according to a manufacture's manual. In brief, 20 μl of a sample solution in water containing CP-Pt was mixed with 200 μl of WST working solution and the reaction was initiated with addition of 20 μl of enzyme working solution. A water soluble WST-1 formazan was spectrophotometrically determined at 450 nm. As a blank, 20 μl of CP-Pt sample solution diluted with 220 μl water was used.

Measurements of uric acid

Because uric acid is the end product from HPX and xanthine after the generation of O_2^- by the enzymatic reaction with XOD, uric acid was assayed to inspect if samples do not inhibit XOD. The concentration of uric acid was spectrophotometrically determined [33]. In brief, the O_2^- generation was started as aforementioned without 15 μl of DMPO and the absorbance at 295 nm was monitored for 10 min. The absorbance of 100 μl of each corresponding sample

solution diluted with 100 μl of 200 mM phosphate buffer (pH 7.5) was subtracted as a blank. Water was used as a control.

Measurements of dissolved oxygen generated from H_2O_2

For measurements of dissolved oxygen (O_2) in water, a galvanic cell oxygen electrode system, DO meter B-505 (Iijima Electronic Corp., Aichi, Japan), was employed [34]. Using a 2 ml semi-sealed chamber purchased with the electrode system, 100 μl of 1 mM CP-Pt or 500 U/ml catalase in water was diluted with 1.7 ml of water. The generation of O_2 was initiated with adding 50 μl of 5 mM H_2O_2. After the generation of O_2 reached to the plateau, 50 μl of 5 mM H_2O_2 was added again. Dissolved O_2 in the reaction mixture was monitored every 3 s.

Data analysis

In all experiments described in this study except for the measurement of the CP-Au/Pt diameter, the number of replicates was three and the data are shown as means ± SD. To estimate the average diameter of CP-Au/Pt, 200 nanoparticles were used. Statistical analysis employed was Student's *t*-test for two sample populations assuming equal variances. Results were taken to be significant if their *P* values were smaller than 0.01.

Results

Characterization of CP-Au/Pt

The CP-Au/Pt were subjected to UV–Vis spectral analysis to estimate the progress of noble metal ion reduction, nanoparticle formation and bimetallic surface structure. Absorption specific to the noble metal precursor ions, sharp absorption of $AuCl_4^-$ at 310 nm or small broad absorption of $PtCl_6^{2-}$ around 370 nm, was not observed in UV–Vis spectra in Figure 1. The UV–Vis spectra also exhibited typical surface plasmon absorption of noble metal nanoparticles. These data indicate that reduction of the noble metal ions was completed and noble metal nanoparticles were composed for the reflux period of 30 min after the addition of citrate. When the percent mole ratio of gold was 50%, typical absorption of gold nanoparticles, even though it was very small, exhibited at 520 nm. This absorption increased as increase of the gold mole ratio. When the percent mole ratio of gold was 75%, the absorption peak shifted to a higher wavelength at 560 nm. However, when the percent mole ratio of gold was 100% (CP-Au), its absorption returned to 520 nm. These data indicate that bimetallic nanoparticles are manufactured and gold atoms may not exist on the surface of CP-Au/Pt when the percent mole ratio of gold is 25%.

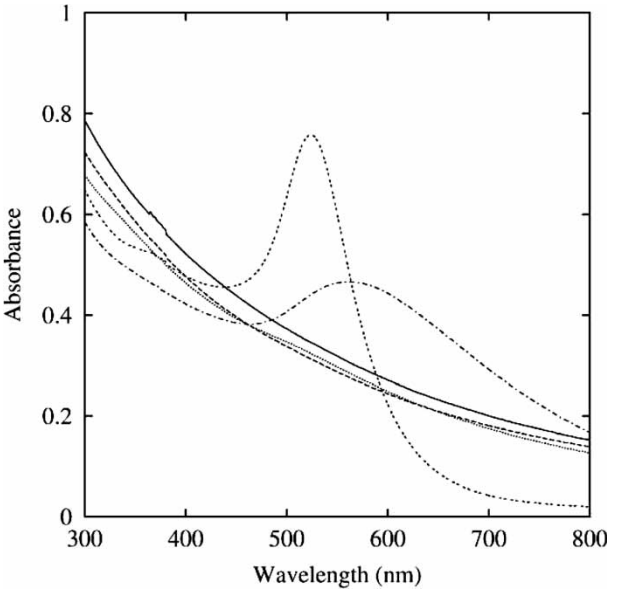

Figure 1. UV–Vis absorption spectra of CP-Au/Pt. Citrate reduction was used to manufacture CP-Au/Pt. The absorption was scanned in the range of the wavelength from 300 to 800 nm by a spectrophotometer. The percent mole ratio of gold to platinum (Au:Pt) was 0:100 (solid line), 25:75 (dashed line), 50:50 (dotted line), 75:25 (dashed-dotted line) and 100:0 (double-dashed line). The concentration of total noble metals was 200 μM in any case.

The actual Au:Pt of CP-Au/Pt and on their surface was estimated by ICP-AES and XPS, respectively. The Au:Pt ratios of CP-Au/Pt and on their surface were similar to those calculated from used materials (Table I). Even when gold was 25%, gold atom was actually present on the surface but its percent mole ratio was slightly but significantly less than those of CP-Au/Pt. When gold was 50%, gold was also significantly less on the surface. These data indicate that CP-Au/Pt have an alloy structure. We analyzed platinum state on the surface of dried CP-Pt and Pt-black powder by XPS. In both cases, platinum was not ionized or oxidized but atom (data not shown).

The CP-Au/Pt were observed under TEM to know their dispersibility and obtain their average diameter.

Table I. Percent mole ratio of gold and platinum.

	Au:Pt (%)	
Preparation	Nanoparticles	Surface
25:75	24 ± 1:76 ± 1	18 ± 2:82 ± 2⋆
50:50	48 ± 1:52 ± 1	45 ± 1:55 ± 1⋆
75:25	74 ± 1:26 ± 1	72 ± 3:28 ± 3

The contents of gold and platinum composing CP-Au/Pt manufactured were analyzed by inductively coupled plasma atomic emission spectrometry (ICP-AES). To estimate the constituent mole ratio of gold and platinum on the surface of CP-Au/Pt, X-ray photoelectron spectroscopy (XPS) was performed using dried CP-Au/Pt on the filter. Values represent mean ± SD of three experiments. ⋆Significantly different from the Au:Pt of nanoparticles ($P < 0.01$).

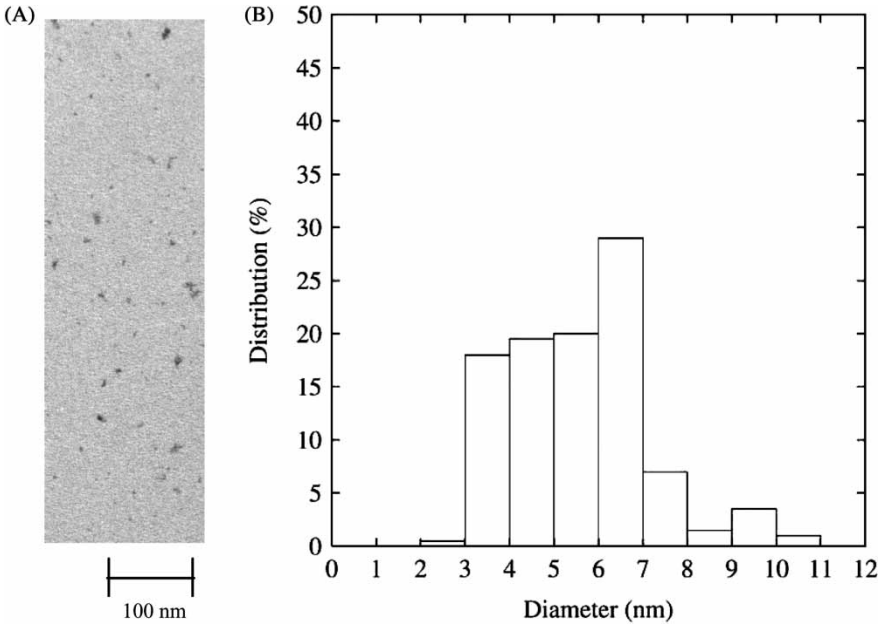

Figure 2. TEM observation of CP-Pt. (A) Transmission electron micrograph. The magnification was 120,000. The concentration of platinum in CP-Pt was 1 mM. (B) Particle size distribution histogram of CP-Pt. The diameter of 200 particles of CP-Pt was measured using enlarged transmission electron micrograph. The average diameter was 4.7 ± 1.5 nm.

A typical TEM micrograph of CP-Pt is shown in Figure 2, panel A. Aggregation of nanoparticles was not observed, showing that CP-Pt are good in dispersion. Other CP-Au/Pt preparations were observed by similar methods. They were also well dispersed without aggregation to speak of (data not shown). The diameter of each particle of CP-Pt in enlarged photographs was measured using a magnifying loupe. The histogram of the particle size distribution is shown in Figure 2, panel B. The most CP-Pt were distributed in the range of 3–10 nm, suggesting that the size of CP-Pt is homogeneous. The average diameter of CP-Pt was 4.7 ± 1.5 nm ($n = 200$). Using similar methods, the average diameters of CP-Au/Pt with 50% platinum and 50% gold and CP-Au were 6.6 ± 1.6 and 12.1 ± 7.0 nm, respectively.

Quenching of H_2O_2

The concentration of total noble metals in CP-Au/Pt was varied from 0 to 200 μM in the sample solution (from 0 to 8 μM in the final reaction mixture). The CP-Au/Pt containing more than 50% platinum quenched H_2O_2 in dose dependent manners as shown in Figure 3, panel A. However, when the percent mole ratio of platinum was less than 25%, H_2O_2 was not quenched. The 50% inhibitory concentration of the ROS generated in the system by CP-Au/Pt (IC_{50}) for H_2O_2 as the final concentration (C_{final}) was 2.2 ± 0.1, 4.0 ± 0.3 and 5.1 ± 0.2 μM of CP-Au/Pt with Au:Pt of 0:100, 25:75 and 50:50, respectively ($n = 3$). Therefore, as the percent mole ratio of platinum was decreased, the quenching activity decreased. The CP-Pt was the strongest quencher. Since CP-Au did not have the quenching activity against H_2O_2, the presence of gold did not enhance the quenching activity of platinum.

Because CP-Pt consist of Pt, citrate and pectin, quenching activity of citrate and pectin was studied to determine which material composing CP-Pt quenches H_2O_2. We also studied the quenching activity of L-ascorbic acid, catechin and Pt-black with the average diameter of 100 nm. The CP-Pt at 100 μM (4 μM as C_{final}) quenched approximately 80% of H_2O_2 whereas 1 mM citrate (40 μM as C_{final}) or 0.06 mg/ml pectin (2.4 μg/ml as C_{final}) did not quench H_2O_2 at all (Figure 3, panel B), showing that the quenching activity of CP-Pt does not belong to citrate or pectin but platinum. None of 100 μM L-ascorbic acid, catechin or Pt-black (4 μM C_{final}) quenched H_2O_2. This means that L-ascorbic acid or catechin does no have strong quenching activity against H_2O_2. Furthermore, when the diameter of platinum particles becomes approximately 10 nm, their quenching activity against H_2O_2 becomes high efficient.

Quenching of O_2^-

Quenching of O_2^- by CP-Au/Pt was measured by ESR using DMPO as a spin-trapping reagent. The DMPO-OOH adduct formed by the reaction of DMPO with O_2^- exhibited tetrad signals as shown in Figure 4(A). We used the intensity of one of four signals indicated by an arrow in the figure to estimate the amount of residual O_2^-. When the concentration of platinum was increased, the signal intensity decreased

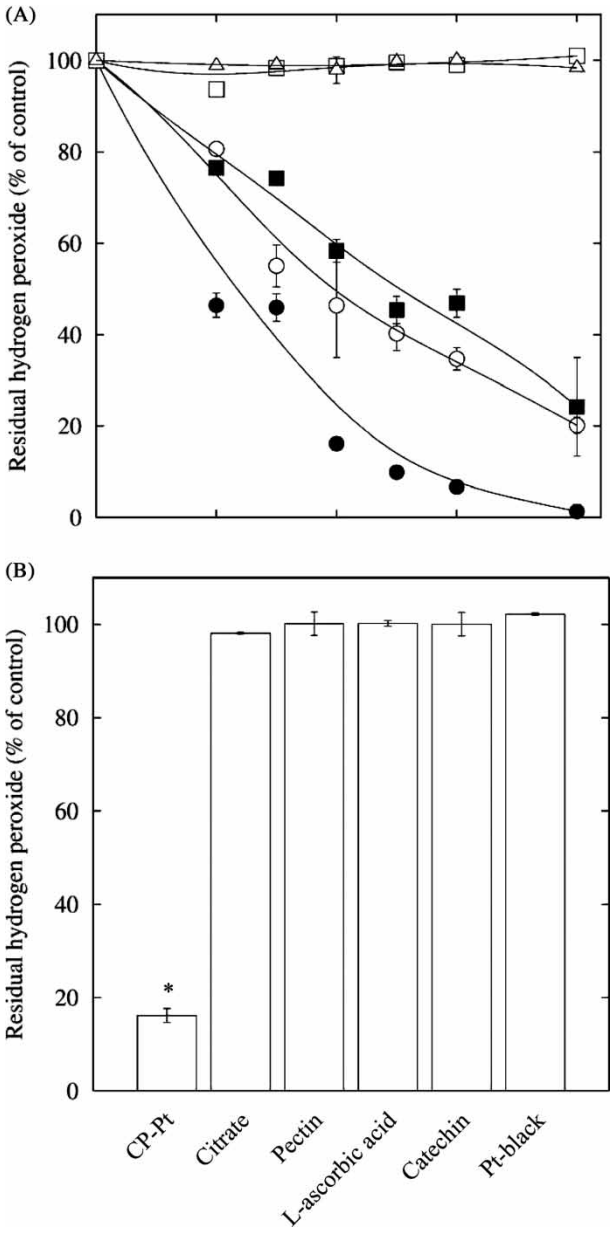

Figure 3. Quenching of H_2O_2 by CP-Au/Pt. (A) Does-dependency. The concentration of residual H_2O_2 was determined by a spectrophotometric method at 240 nm after 5 min incubation. The concentration of total noble metals in CP-Au/Pt was varied from 0 to 200 μM in 120 μl of sample solution before mixing with 2880 μl of 20 mM H_2O_2 (from 0 to 8 μM in the final reaction mixture). Values represent means ± SD of three experiments. Au:Pt = 0:100, closed circle; 25:75, open circle; 50:50, closed square; 75:25, open square; 100:0, open triangle. (B) Comparison of quenching activity. The concentration of platinum in CP-Pt, L-ascorbic acid, catechin and Pt-black was 100 μM in the sample solution (4 μM as C_{final}). The concentrations of citrate and pectin were 1 mM and 0.06 mg/ml, respectively, in the sample solution (40 μM and 2.4 μg/ml, respectively, as C_{final}). Values represent means ± SD of three experiments. *Significantly different from the control ($P < 0.01$).

as shown in Figure 4(B),(C), suggesting that platinum may quench O_2^-.

The concentration of noble metals in CP-Au/Pt was varied from 0 to 500 μM in the sample solution (from 0 to 233 μM in the final reaction mixture).

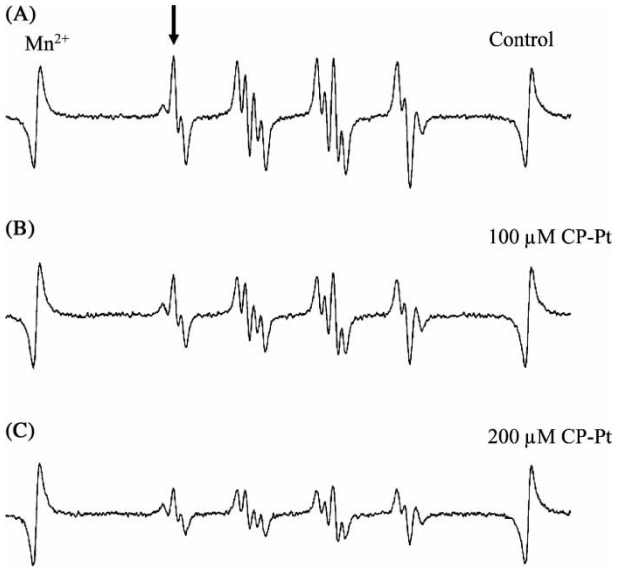

Figure 4. ESR spectra of DMPO—OOH. The O_2^- was generated by an enzymatic reaction with HPX and XOD. The ESR signal intensity indicated by an arrow was converted to numeric values by normalizing with the signal intensity of Mn^{2+} marker. The concentration of platinum in CP-Pt was 0 μM (panel A), 100 μM (panel B) and 200 μM (panel C) in 100 μl of sample solution before making reaction mixture (0, 46.5 and 93 μM, respectively, as C_{final}).

All the CP-Au/Pt quenched O_2^- in dose dependent manners as shown in Figure 5, panel A. Among CP-Au/Pt tested, CP-Pt was the strongest quencher. When the percent mole ratio of gold was increased in CP-Au/Pt, the quenching activity decreased. The IC_{50} for O_2^- as C_{final} was 72 ± 6, 98 ± 7 and 147 ± 10 μM of CP-Au/Pt with Au:Pt of 0:100, 25:75 and 50:50, respectively ($n = 3$). When the Au:Pt ratios were 75:25 and 100:0, we could not determine their IC_{50} because O_2^- was not quenched by far more than 50% in the range of 0–500 μM (from 0 to 233 μM as C_{final}). These data suggest that platinum quenches more effectively O_2^- than gold. The presence of gold in CP-Au/Pt did not enhance the quenching activity of platinum against O_2^-, too.

To determine which material composing CP-Pt quenches O_2^-, quenching activity of citrate and pectin was tested. In this experiment, we also tested tannic acid in addition to L-ascorbic acid, catechin and Pt-black. Because tannic acid is a representative inhibitor of XOD (33), it may exhibit apparent quenching of O_2^- due to decrease of O_2^- generation. The CP-Pt at 200 μM (93μM as C_{final}) quenched O_2^- approximately 60% whereas 2 mM citrate (0.93 mM as C_{final}) or 0.12 mg/ml pectin (0.056 mg/ml as C_{final}) failed to quench O_2^-, showing that platinum has the quenching activity (Figure 5, panel B). Two hundred micrometer L-ascorbic acid, 200 μM catechin and 0.04 mg/ml tannic acid (93μM, 93μM and 18.6 μg/ml, respectively, as C_{final}) quenched O_2^- more effectively than 200 μM platinum in CP-Pt

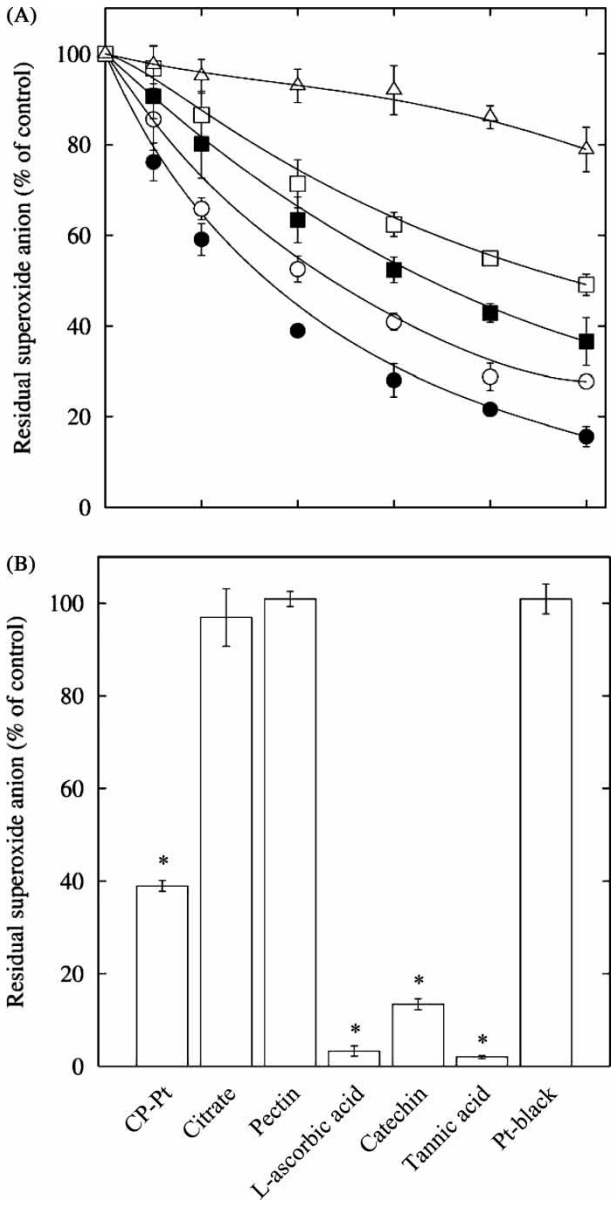

Figure 5. Quenching of O_2^- by CP-Au/Pt. (A) Does-dependency. Residual O_2^- was expressed by percent of the control numeric value normalized by Mn^{2+} marker. For control, water was used. The concentration of total noble metals in CP-Au/Pt was varied from 0 to 500 μM in sample solution (0–233 μM as C_{final}). Values represent means ± SD of three experiments. Au:Pt = 0:100, closed circle; 25:75, open circle; 50:50, closed square; 75:25, open square; 100:0, open triangle. (B) Comparison of quenching activity. The concentration of CP-Pt, L-ascorbic acid and Pt-black was 200 μM in sample solution (93 μM as C_{final}). The concentrations of tri-sodium citrate, pectin and tannic acid were 2 mM, 0.12 and 0.04 mg/ml, respectively, in the sample solution (0.93 mM, 0.056 mg/ml and 18.6 μg/ml, respectively, as C_{final}). Values represent means ± SD of three experiments. *Significantly different from the control ($P < 0.01$).

(93μM as C_{final}). However, 200 μM Pt-black (93μM as C_{final}) did not quench O_2^- at all.

Because tannic acid exhibited apparent quenching of O_2^-, it is possible to speculate that CP-Au/Pt showed apparent quenching of O_2^- via the inhibition of XOD. To make it sure that CP-Pt do not inhibit XOD, the production of uric acid which is the end product of HPX after generation of O_2^- was monitored for 10 min. Platinum in CP-Pt at 200 μM (100 μM as C_{final}) did not decrease the production of uric acid, showing that CP-Pt do not inhibit XOD (Figure 6). However, 0.04 mg/ml tannic acid (20 μg/ml as C_{final}) considerably decreased the production of uric acid. Apparent quenching of O_2^- by tannic acid observed in Figure 5, panel B seems to be due to decrease of O_2^- generation by inhibition of XOD. L-ascorbic acid at 200 μM (100 μM as C_{final}) inhibited XOD to a significant extent, suggesting that L-ascorbic acid not only quenches O_2^- but also decreases O_2^- generation.

Because the DMPO—OOH adduct is instable, CP-Au/Pt may facilitate the degradation or reduction of the adduct to an ESR-silent species, instead of the quenching of O_2^-. Therefore, we determined O_2^- by a different method, formazan formation using a SOD assay kit-WST to confirm the quenching activity of CP-Au/Pt against O_2^-. The production of WST-1 formazan increased with incubation time and 100 μM platinum in CP-Pt (8.33 μM as C_{final}) decreased this time-dependent formazan production (Figure 7, panel A). The concentration of platinum in CP-Pt was varied from 0 to 200 μM in the sample solution (from 0 to 16.7 μM in the final reaction mixture). The CP-Pt decreased the formazan produced for 10 min

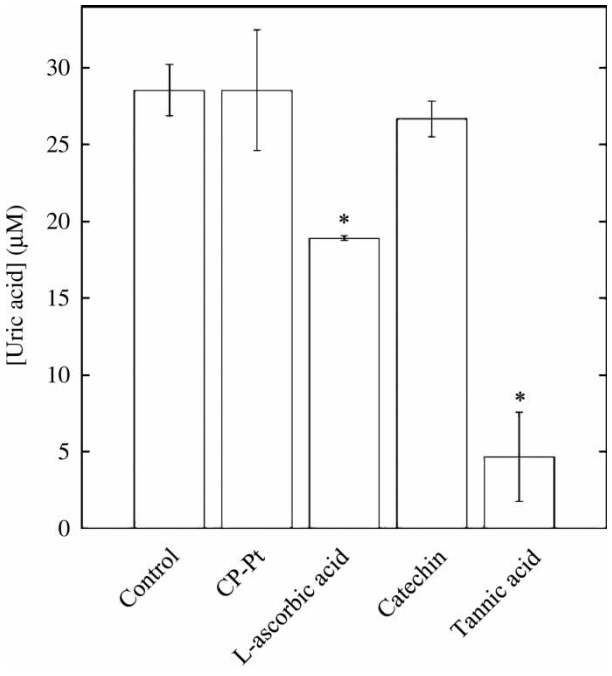

Figure 6. Measurements of XOD activity. The concentration of uric acid was determined by a spectrophotometric method (295 nm). The amount of uric acid produced for 10 min was calculated. The concentration of platinum in CP-Pt, L-ascorbic acid and catechin was 200 μM in sample solutions (100 μM as C_{final}). The concentration of tannic acid was 0.04 mg/ml in the sample solution (0.02 mg/ml as C_{final}). Values represent means ± SD of three experiments. *Significantly different from the control ($P < 0.01$).

in a dose-dependent manner (Figure 7, panel B). Since CP-Pt do not inhibit XOD, CP-Pt quenched O_2^- to decrease formazan production. This result strongly indicates that quenching of O_2^- by CP-Au/Pt observed in the ESR experiments is due to actual quenching of O_2^- rather than degradation or reduction of the DMPO—OOH adduct to an ESR-silent species.

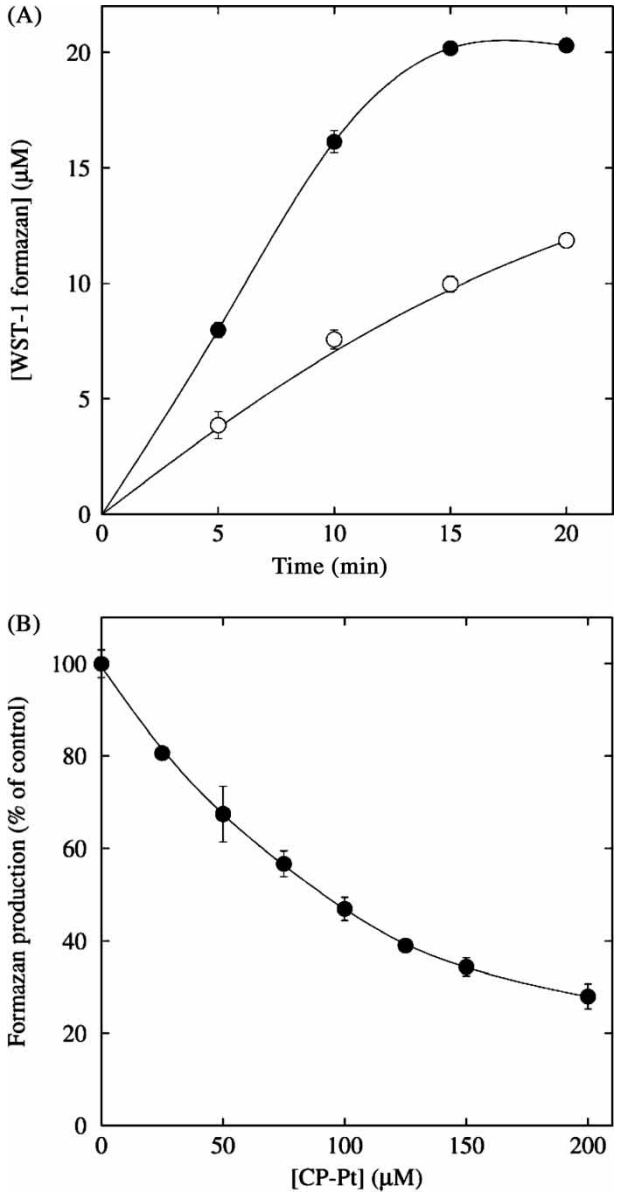

Figure 7. Inhibition of formazan formation by CP-Pt. A SOD assay kit-WST was used. Assay was performed according to a manufacture's manual. The O_2^- was generated by the enzymatic reaction with xanthine and XOD. A water soluble WST-1 formazan was spectrophotometrically determined at 450 nm. (A) The concentration of platinum in CP-Pt was 100 μM in the sample solution (8.33 μM as C_{final}). Values represent means ± SD of three experiments. Control, closed circle; CP-Pt, open circle. (B) The concentration of platinum in CP-Pt was varied from 0 to 200 μM in the sample solution (0–16.7 μM as C_{final}). Water was used as a vehicle control and WST-1 formazan production was expressed as percentage of the control. Values represent means ± SD of three experiments.

The result also suggests that CP-Pt may quench O_2^- like SOD.

Catalytic quenching properties of CP-Au/Pt

To examine if nanosized platinum works as a catalyst like catalase when CP-Pt quenches H_2O_2, dissolved oxygen was monitored using an oxygen electrode. Each time 50 μl of 5 mM H_2O_2 was added as indicated by arrows in Figure 8, oxygen generation was observed in the presence of CP-Pt (Figure 8, panel A). A similar experiment was performed with catalase and a similar repeating oxygen generation after H_2O_2 addition was observed. These data indicate that nanosized platinum catalytically decomposes H_2O_2 like catalase and consequently generate oxygen.

The time course of residual O_2^- was monitored in the presence of CP-Pt to examine if quenching activity of CP-Pt against O_2^- persists like SOD. The concentrations of platinum in CP-Pt, L-ascorbic acid and SOD were adjusted to quench O_2^- to a similar extent without incubation. Their concentrations were 200 μM, 50 μM and 0.2 U/ml, respectively, in sample solutions (100 μM, 25 μM and 0.1 U/ml, respectively, during the incubation). The CP-Pt and SOD continuously quenched O_2^- for 30 min whereas L-ascorbic acid quenched O_2^- only for 10 min (Figure 8, panel B). Once L-ascorbic acid quenches O_2^-, L-ascorbic acid is oxidized so as to loose its quenching activity. However, the quenching activity of CP-Pt persisted for 30 min even thought the quenching activity was equal to that of L-ascorbic acid at zero time. These data indicate that CP-Pt may catalytically quench O_2^- like SOD.

Discussion

We started this research to take it into consideration to use noble metal nanoparticles in biological experiments with living cells and animal models of diseases in the future. Strong reducing reagents usually used in chemical methods to prepare metal nanoparticles are ethanol, hydrazine monohydrate, sodium tetrahydroborate and so on. But some of them are supposed to be toxic to living things if they are contaminated after synthesis of metal nanoparticles. For the reason, citrate and ethanol are applicable to manufacture noble metal nanoparticles for biological use. We chose citrate because it is inexpensive and also serves as a stabilizer for noble metal nanoparticles. We could make stable dispersion of bimetallic nanoparticles containing gold and platinum in water by reducing $AuCl_4^-$ and $PtCl_6^{2-}$ with citrate as described by Frens [30]. However, these noble metal nanoparticles were not stable in an isotonic salt solution. They aggregated, composed larger particles and precipitated in 0.9% NaCl overnight. Because oligosaccharides like β-cyclodextrin are often used as

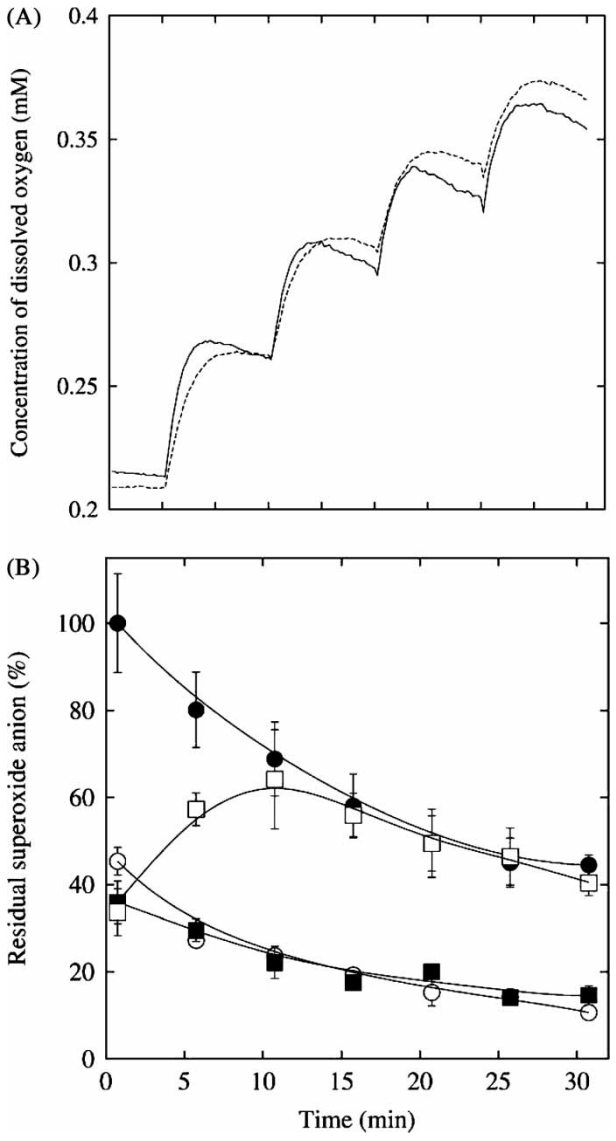

Figure 8. Catalytic activity of CP-Pt. (A) Generation of O_2 from H_2O_2 in the presence of CP-Pt. Generation of O_2 was initiated with the first addition of 50 μl of 5 mM H_2O_2. Generated O_2 monitored by the oxygen electrode. Every 120 s 50 μl of 5 mM H_2O_2 was added three more times as indicated by arrows in the figure. The final concentrations of platinum in CP-Pt (solid line) and catalase (dashed line) were 50 μM and 25 U/ml, respectively, in the reaction mixture after the forth addition of H_2O_2. (B) Time course of residual O_2^-. Fifty microlitre of 5.5 mM HPX was mixed with 100 μl of a sample solution. Generation of O_2^- was initiated by adding 50 μl of 0.2 U/ml XOD and incubated for predetermined periods. Subsequently, 15 μl of 8.8 M DMPO was added to the reaction mixture and 45 s later ESR measurements were performed. The concentrations of platinum in CP-Pt, L-ascorbic acid and SOD were 200 μM, 50 μM and 0.2 U/ml, respectively, in the sample solution (100 μM, 25 μM and 0.1 U/ml, respectively, during the incubation before adding DMSO). Values represent means ± SD of three experiments. Control, closed circle; CP-Pt, open circle; SOD, closed square; L-ascorbic acid, open square.

protecting reagents [35], we examined if pectin, which is a food additive, improves the stability of the noble metal nanoparticles in 0.9% NaCl. After the noble metal nanoparticles were made and the reaction mixture was cooled down to the room temperature, pectin was dissolved in the dispersion, NaCl was further added to give the isotonicicity and the resultant mixture was maintained. The stability of the noble metal nanoparticles was dramatically improved. Consequently, in this study, we used bimetallic nanoparticles consisting of gold and platinum which were prepared by citrate reduction and complementarily stabilized with pectin (CP-Au/Pt). Approximately 1 year past after preparation of nanoparticles but no precipitation has not been observed in CP-Au/Pt solution so far.

Before citrate reflux the reaction mixture was light yellow due to $AuCl_4^-$ and $PtCl_6^{2-}$. When the reaction mixture contained only $AuCl_4^-$, the color of the mixture was getting darker as soon as citrate was added. This means that the reduction of gold ions started right after the addition of citrate. In the case of platinum, it took approximately 15 min till the ion reduction started. According to the result of the UV–Vis spectrum measurement, absorption spectra specific to noble metal precursor ions, sharp absorption of $AuCl_4^-$ at 310 nm or small broad absorption of $PtCl_6^{2-}$ around 370 nm, were not observed after 30 min reflux with citrate (Figure 1). Therefore, we judged that the reflux with citrate at 100°C for 30 min was enough to reduce noble metal ions to atoms. The size of metal nanoparticles depends on the refluxing period. The diameters of CP-Pt, CP-Au/Pt containing 50% platinum and 50% gold and CP-Au were 4.7 ± 1.5, 6.6 ± 1.6 and 12.1 ± 7.0 nm, respectively (Figure 2, panel B). When we manufactured platinum nanoparticles protected with poly (acrylic acid) by reducing for 2 h with ethanol (PAA-Pt), their diameter was 2.0 ± 0.4 nm ($n = 200$). The diameter of gold nanoparticles protected with chitosan by 1 h reduction with sodium tetrahydroborate was in the range of 5–15 nm [16]. To take it into consideration that polymers more effectively restrict metal aggregation to lessen the size of nanoparticles, we thought that 30 min reflux with citrate were not too long.

When the percent mole ratio of gold was 25%, the spectrum of CP-Au/Pt did not show the peak specific to gold nanoparticles but was similar to that of CP-Pt, indicating that gold may not be present on the surface of CP-Au/Pt (Figure 1). This result coincides with former reports [1,36]. However, XPS analysis shows that CP-Au/Pt have an alloy structure and gold is present on the surface of CP-Au/Pt with 25% even though the percent mole ratio of gold is slightly but significantly low (Table I). When the percent mole ratio of gold was more than 50%, the spectrum exhibited a typical absorption of gold nanoparticles (Figure 1). The peak of this absorption was shifted to higher wavelength at 560 nm when the percent ration of gold was 75% (Figure 1). The cause of this peak shift is unknown but a similar shift is reported

previously [1,36]. When bimetallic nanoparticles consisting of 20 and 40% platinum protected with poly(ethylene glycol)monolaurate were prepared by alcohol reduction, the peak shift was not observed [29]. The shift seems to occur due to protecting reagents and/or reduction methods. This means that the surface plasmon absorption of bimetallic nanoparticles consisting of 75% gold and 25% platinum may depend on their alloy structure altered by protecting reagents and/or reduction methods.

We studied quenching activity and properties of CP-Au/Pt against H_2O_2 and O_2^-. It is well known that large pieces of platinum such as platinum powder decompose two moles of H_2O_2 to one moles of O_2 and two moles of H_2O [37]. While 100 μM CP-Pt (4 μM as C_{final}) quenched H_2O_2, Pt-black at the same concentration did not (Figure 3, panel B). This result indicates that because platinum state of the surface of CP-Pt and Pt-black was atomic, the catalytic activity of CP-Pt is high due to the largeness of its total surface per mole. If CP-Pt and Pt-black are globate and the number of platinum atoms per space is unvarying in CP-Pt and Pt-black, the surface of CP-Pt is calculated to be approximately 20 times larger than that of Pt-black using their average diameters of 5 and 100 nm. If this surface ratio is right, Pt-black is supposed to quench 4% of H_2O_2 because CP-Pt at 100 μM (4 μM as C_{final}) quenched approximately 80% of H_2O_2 (Figure 3, panel B). To determine the actual surface area ratio of CP-Pt and Pt-black, a carbon monoxide pulse method was performed. However, we failed because protecting reagents, citrate and pectin, disturbed to estimate the surface area of CP-Pt. We think that though Pt-black has the quenching activity against H_2O_2, its concentration of 100 μM (4 μM as C_{final}) was not enough to show a significant quenching. Quenching of H_2O_2 decreased as the percent mole ratio of platinum was decreased. When the percent mole ratio of platinum was less than 25%, H_2O_2 was not quenched (Figure 3, panel A). Even though platinum atoms exist on the surface of CP-Au/Pt with 75% gold and 25% platinum (Table I), they are supposed not to enough to catalyze the decomposing reaction of H_2O_2. The CP-Au did not quench H_2O_2. In the case of H_2O_2 quenching, gold does not help increase the quenching activity of platinum. We also showed generation of O_2 in the presence of CP-Pt whenever H_2O_2 was added (Figure 8, panel A). Platinum diminished to approximately 10 nm quenches H_2O_2 much more efficiently than larger pieces of platinum.

In this study, we showed quenching of O_2^- by CP-Au/Pt for the first time (Figure 5, panel A). The quenching manner of O_2^- by CP-Au/Pt was dose-dependent. Because CP-Pt quenched much more effectively than CP-Au, the quenching activity of platinum seems to be stronger than that of gold. In the case of O_2^- quenching, the presence of gold did not help increase the quenching activity of platinum, too. Pt-black did not quench O_2^- (Figure 5, panel B). To our knowledge, there is no report with regard to quenching of O_2^- by platinum. PAA-Pt with the diameter of 2 nm also quenched O_2^- as well as H_2O_2. The quenching activity of platinum against O_2^- may be generated or become efficient when it is made small to approximately 10 nm. We assayed the residual O_2^- by ESR to know the quenching activity of samples. If they inhibit XOD and consequently decrease the generation of O_2^-, we may mistake the inhibition of XOD for the quenching of O_2^-. To get rid of this misjudgement, we assayed uric acid. The CP-Pt did not decrease the production of uric acid but tannic acid, a representative inhibitor of XOD, did (Figure 6). As a result, CP-Au/Pt seem to quench O_2^-, instead of decrease of O_2^- production by inhibition of XOD. Interestingly, L-ascorbic acid decreased the production of uric acid to a significant extent. We checked the disturbance of uric acid absorption by L-ascorbic acid and found that the disturbance was almost negative (data not shown). This result strongly suggests that L-ascorbic acid inhibits the activity of XOD. Therefore, when we estimate the quenching activity of L-ascorbic acid against O_2^- generated by an enzymatic reaction with XOD, we have to take account of the decrease of O_2^- generation via inhibition of XOD. In L-ascorbic acid, it is well known that this acid reduces nitroxide spin adducts [38]. Therefore, to make it sure that the quenching activity of CP-Au/Pt observed in the ESR experiments is not due to their facilitation of degradation or reduction of the DMPO—OOH adduct to an ESR silent species, we determined O_2^- by a different method, formazan formation using a kit for assaying SOD-like activity of substances. Formazan production was dose-dependently decreased by CP-Pt (Figure 7, panel B). When CP-Pt was added to the reaction mixture after WST-1 formazan was formed and its absorbance reached the plateau, CP-Pt did not decrease the absorbance, indicating that CP-Pt do not decompose the formazan (data not shown). Because CP-Pt do not inhibit XOD, CP-Pt quench O_2^-. This result strongly indicates that quenching of O_2^- by CP-Au/Pt observed in the ESR experiments is due to actual quenching of O_2^-, instead of degradation or reduction of the adduct to an ESR-silent species. We wanted to examine if L-ascorbic acid decreases formazan formation using this kit but failed because the WST working solution became yellow by mixing with L-ascorbic acid. Therefore, it is still unclear whether L-ascorbic acid may facilitate the degradation of the DMPO—OOH adduct. We also studied the time course of O_2^- quenching by CP-Pt and showed persistence of O_2^- quenching by CP-Pt similar to that by SOD while L-ascorbic acid lost its quenching activity for 10 min (Figure 8, panel B). Because CP-Pt actually quench O_2^-, which is verified by a SOD assay

kit, and this quenching activity persists like SOD, CP-Au/Pt may catalyze a disproportionate reaction of decomposing O_2^- to O_2 and H_2O_2 like SOD though produced H_2O_2 is subsequently decomposed to O_2 and H_2O. To approach the mechanisms of how CP-Au/Pt quench O_2^-, we tried to monitor O_2 derived from O_2^- quenching by CP-Au/Pt using an oxygen electrode but failed due to excessive generation of O_2 by decomposition of H_2O_2 generated by HPX and XOD. From our results obtained in this study, it is not still enough to definitely say that CP-Au/Pt are catalysts of O_2^-, because the precise mechanisms of O_2^- quenching by CP-Au/Pt are left unsolved. Further investigations are required.

To remove excessive H_2O_2 and O_2^- in the body, platinum monometallic nanoparticles seem to be the strongest tool so far. We expected help of gold in platinum bimetallic nanoparticles to enhance the quenching activity in ROS quenching like in the case of hydrogenation and hydrogen evolution [28,29]. Gold and palladium are usually thought to change electric properties of platinum on the surface of metal nanoparticles and increase the catalytic activity. But, our speculation was not right in the case of ROS. The CP-Au/Pt manufactured in this study were alloy-structured (Table I). Therefore, gold may increase the ROS-quenching activity when bimetallic nanoparticles consist of gold and platinum are core/shell structured. We also need to investigate effects of palladium on ROS quenching activity of platinum nanoparticles. To find a stronger quencher of ROS, materials and the structure of metal nanoparticles are necessary to study in details. But, the current study still shows the usefulness of gold in nanoparticles. The CP-Au/Pt with 25% gold and 75% platinum could quench both ROS, H_2O_2 and O_2^-, even though their quenching activity was a little smaller than that of CP-Pt (Figure 3, panel A and Figure 5, panel A). Therefore, to equip nanoparticles with biological function by binding small peptides to their surface, gold on the surface of metal nanoparticles will be useful.

To our knowledge, among inorganic nanoparticles, only gold nanoparticles and nano red elemental selenium (nano-Se) have been reported their anti-oxidant effects (16–18, 39). In the case of gold nanoparticles, their quenching activity only against hydroxyl radical has been shown. Quenching activity of gold nanoparticles against H_2O_2 and O_2^- were investigated in the current study. Nano-Se possess quenching activity of free radicals including O_2^-. Small nano-Se (5–15 nm) quenched free radicals effectively. The IC_{50} for O_2^- by small nano-Se was 44 μM. However, small nano-Se are stabilized with huge amount of bovine serum albumin (BSA), and elemental Se and BSA were inseparable. Because BSA itself is an antioxidant, it is not clear which materials, Se or BSA, quenches free radicals, how much percent of free radicals are quenched by Se, or how interaction between elemental Se and BSA enhances the scavenging activity of elemental Se. To elucidate these questions, more experiments are required. Furthermore, to manufacture nano-Se, sodium serenite was used. This reagent is very toxic. Therefore, though selenium is one of the essential metal in the body, sodium serenite as contamination of nano-Se makes it difficult to use in biological purposes. Salen manganese complexes such as EUK-8 and -134 are only the SOD/catalase mimetics so far reported [40,41]. These compounds have proven efficacious against a variety of oxidative stress diseases [41–43]. Furthermore, recent papers have shown that they are effective to extend life-span of *Caenorhabditis elegans* and mouse [44,45]. In the current study, we characterized the quenching activity of CP-Au/Pt against H_2O_2 and O_2^-, indicating that CP-Au/Pt containing platinum more than 50% may be a kind of SOD/catalase mimetic. The SOD activity was 4640, 370 and 142 U/mg in SOD we used, EUK-8 (IC_{50} of $O_2^- = 1.5\,\mu M$ and MW = 374.4 from [45]) and CP-Pt, respectively and the catalase activity was 11,500, 0.6 and 8317 U/mg in catalase we used, EUK-8 [40] and CP-Pt, respectively. This comparison indicates that enzymes themselves are the strongest quenchers but CP-Pt have much higher quenching activity of H_2O_2 than EUK-8. Therefore, CP-Pt may be effective in oxidative stress diseases and aging.

References

[1] Toshima N, Yonezawa T. Bimetallic nanoparticles-novel materials for chemical and physical applications. New J Chem 1998;22:1179–1201.

[2] Aiken-III JD, Finke RG. A review of modern transition-metal nanoclusters: Their synthesis, characterization, and applications in catalysis. J Mol Catal A Chem 1999;145:1–44.

[3] Roucoux A, Schulz J, Patin H. Reduced transition metal colloids: A novel family of reusable catalysts? Chem Rev 2002;102:3757–3778.

[4] Bradley JS, Schmid G. Noble metal nanoparticles. In: Schmid G, editor. Nanoparticles from theory to application. Weinheim: Willy-VCH; 2004. p 186-199–230-238.

[5] Toshima N, Shiraishi Y, Teranishi T, Miyake M, Tominaga T, Watanabe H, Brijoux W, Bönnemann H, Schmid G. Various ligand-stabilized metal nanoclusters as homogeneous and heterogeneous catalysts in the liquid phase. Appl Organometal Chem 2001;15:178–196.

[6] Toshima N, Yamaji Y, Teranishi T, Yonezawa T. Photo-sensitized reduction of carbon dioxide in solution using noble-metal clusters for electron transfer. Z Naturforsch 1995;50: 283–291.

[7] Shiraishi Y, Toshima N. Colloidal silver catalysts for oxidation of ethylene. J Mol Catal A Chem 1999;141:187–192.

[8] Lewis LN, Lewis N. Platinum-catalyzed hydrosilylation-colloid formation as the essential step. J Am Chem Soc 1986;108:7228–7231.

[9] Yadav OP, Palmqvist A, Cruise N, Holmberg K. Synthesis of platinum nanoparticles in microemulsions and their catalytic activity for the oxidation of carbon monoxide. Colloids Surf A Physicochem Eng Asp 2003;221:131–134.

[10] Sun S, Murray CB, Weller D, Folks L, Moser A. Monodisperse FePt nanoparticles and ferromagnetic FePt nanocrystal superlattices. Science 2000;287:1989–1992.
[11] Park J, Cheon J. Synthesis of "solid solution" and "core-shell" type cobalt-platinum magnetic nanoparticles via transmetalation reactions. J Am Chem Soc 2001;123:5743–5746.
[12] Schmid G, Chi LF. Metal clusters and colloids. Adv Mater 1998;10:515–526.
[13] Lewis LN. Chemical catalysis by colloids and clusters. Chem Rev 1993;93:2693–2730.
[14] Henglein A. Small-particle research: Physicochemical properties of extremely small colloidal metal semiconductor particles. Chem Rev 1989;89:1861–1873.
[15] Mannweiler K, Hohenberg H, Bohn W, Rutter G. Protein—A gold particles as markers in replica immunocytochemistry: High resolution electron microscope investigations of plasma membrane surfaces. J Microsc 1982;126:145–149.
[16] Esumi K, Takei N, Yoshimura T. Antioxidant-potentiality of gold–chitosan nanocomposites. Colloids Surf B Biointerfaces 2003;32:117–123.
[17] Esumi K, Houdatsu H, Yoshimura T. Antioxidant action by gold-PAMAM dendrimer nanocomposites. Langmuir 2004; 20:2536–2538.
[18] Akiyama S, Yoshimura T, Esumi K. Antioxidant activity of noble metal (gold, platinum)—biopolymer nanocomposites. J Jpn Soc Colour Mater 2005;78:112–121.
[19] Halliwell B, Gutteridge JMC. The chemistry of free radicals and related "reactive species". In: Halliwell B, Gutteridge JMC, editors. Free radicals in biology and medicine. 3rd ed. New York: Oxford; 1999. p 36–104.
[20] Raha S, Robinson BH. Mitochondria, oxygen free radicals, disease and aging. Trends Biochem Sci 2000;25:502–508.
[21] Halliwell B, Gutteridge JMC. Antioxidant defences. In: Halliwell B, Gutteridge JMC, editors. Free radicals in biology and medicine. 3rd ed. New York: Oxford; 1999. p 105–245.
[22] Bokov A, Chaudhuri A, Richardson A. The role of oxidative damage and stress in aging. Mech Ageing Dev 2004;125: 811–826.
[23] Halliwell B, Gutteridge JMC. Free radicals, other reactive species and disease. In: Halliwell B, Gutteridge JMC, editors. Free radicals in biology and medicine. 3rd ed. New York: Oxford; 1999. p 617–783.
[24] Finkel T. Redox-dependent signal transduction. FEBS Lett 2000;476:52–54.
[25] Klotz L-O. Oxidant-induced signaling: Effects of peroxynitrite and singlet oxygen. Biol Chem 2002;383:443–456.
[26] Stamler JS, Lamas S, Fang FC. Nitrosylation: The prototypic redox-based signaling mechanism. Cell 2001;106:675–683.
[27] Hampton MB, Kettle AJ, Winterbour CC. Inside the neutrophil phagosome: Oxidants, myeloperoxidase, and bacterial killing. Blood 1998;92:3007–3017.
[28] Toshima N, Shiraishi Y, Shitotsuki A, Ikaenaga D, Wang Y. Novel synthesis, structure and catalysis of inverted core/shell structured Pd/Pt bimetallic nanoclusters. Eur Phys J D 2001; 16:209–212.
[29] Yonezawa T, Toshima N. Polymer- and micelle-protected gold/platinum bimetallic systems: Preparation, application to catalysis for visible-light-induced hydrogen evolution, and analysis of formation process with optical methods. J Mol Catal 1993;83:167–181.
[30] Frens G. Controlled nucleation for the regulation of the particle size in monodisperse gold suspensions. Nature Phys Sci 1973;241:20–22.
[31] Ueno S, Iwasaka M. Catalytic activity of catalase under strong magnetic fields of up to 8 T. J Appl Phys 1996;79:4705–4707.
[32] Koide T, Noda H, Liu W, Ogata T, Kamada H. Determination of superoxide scavenging activity of a sample containing xanthine oxidase inhibitor by ESR spin trapping. Anal Sci 2000;16:1029–1032.
[33] Hatano T, Yasuhara T, Yoshihara R, Agata I, Noro T, Okuda T. Effects of interaction of tannins with co-existing substances. VII. Inhibitory effects of tannins and related polyphenols on xanthine oxidase. Chem Pharm Bull 1990;38:1224–1229.
[34] Long LH, Evans PJ, Halliwell B. Hydrogen peroxide in human urine: Implications for antioxidant defense and redox regulation. Biochem Biophys Res Commun 1999;262: 605–609.
[35] Alvarez J, Liu J, Román E, Kaifer AE. Water-soluble platinum and palladium nanoparticles modified with thiolated β-cyclodextrin. Chem Commun 2000;13:1151–1152.
[36] Miner RS, Jr, Namba S, Turkevich J. Synthesis, characteristics and catalytic activity of monodispersed platinum alloys with gold and palladium. Stud Surf Sci Catal 1981;7:160–172.
[37] Kobozev NI. Catalase action of various catalysts. The catalytic activity and structure. Acta Phys Chim URSS 1946;21: 469–518.
[38] Yu Z, Kotake Y, Janzen EG. Structural dependence of nitroxide spin labels and nitroxide spin adducts on their reducibility by ascorbate ion. Redox Rep 1996;2:133–139.
[39] Huang B, Zhang J, Hou J, Chen C. Free radical scavenging efficiency of nano-Se *in vitro*. Free Radic Biol Med 2003;35: 805–813.
[40] Baudry M, Etienne S, Bruce A, Palucki M, Jacobsen E, Malfroy B. Salen–manganese complexes are superoxide dismutase-mimics. Biochem Biophys Res Commun 1993; 192:964–968.
[41] Baker K, Marcus CB, Huffman K, Kruk H, Malfroy B, Doctrow SR. Synthetic combined superoxide dismutase/catalase mimetics are protective as a delayed treatment in a rat stroke model: A key role for reactive oxygen species in ischemic brain injury. J Pharmacol Exp Ther 1998;284:215–221.
[42] Doctrow SR, Huffman K, Marcus CB, Musleh W, Bruce A, Baudry M, Malfroy B. Salen–manganese complexes: Combined superoxide dismutase/catalase mimics with broad pharmacological efficacy. Adv Pharmacol 1997;38:247–269.
[43] Jung C, Rong Y, Doctrow S, Baudry M, Malfroy B, Xu Z. Synthetic superoxide dismutase/catalase mimetics reduce oxidative stress and prolong survival in a mouse amyotrophic lateral sclerosis model. Neurosci Lett 2001;304:157–160.
[44] Melov S, Ravenscroft J, Malik S, Gill Ms, Walker DW, Clayton PE, Wallace DC, Malfroy B, Doctrow SR, Lithbow GJ. Extension of life-span with superoxide dismutase/catalase mimetics. Science 2000;289:1567–1569.
[45] Melov S, Doctrow SR, Schneider JA, Haberson J, Manisha P, Coskun PE, Huffman K, Wallace DC, Malfroy B. Life extension and rescue of spongiform encephalopathy in superoxide dismutase 2 nullizygous mice treated with superoxide dismutase–catalase mimetics. J Neurosci 2001;21: 8348–8353.